

The 2dF Galaxy Redshift Survey: luminosity dependence of galaxy clustering

Peder Norberg,^{1*} Carlton M. Baugh,¹ Ed Hawkins,² Steve Maddox,² John A. Peacock,³ Shaun Cole,¹ Carlos S. Frenk,¹ Joss Bland-Hawthorn,⁴ Terry Bridges,⁴ Russell Cannon,⁴ Matthew Colless,⁵ Chris Collins,⁶ Warrick Couch,⁷ Gavin Dalton,⁸ Roberto De Propris,⁷ Simon P. Driver,⁹ George Efstathiou,¹⁰ Richard S. Ellis,¹¹ Karl Glazebrook,¹² Carole Jackson,⁵ Ofer Lahav,¹⁰ Ian Lewis,⁴ Stuart Lumsden,¹³ Darren Madgwick,¹⁰ Bruce A. Peterson,⁵ Will Sutherland³ and Keith Taylor^{4,11}

¹*Department of Physics, University of Durham, South Road, Durham DH1 3LE*

²*School of Physics & Astronomy, University of Nottingham, Nottingham NG7 2RD*

³*Institute for Astronomy, University of Edinburgh, Royal Observatory, Blackford Hill, Edinburgh EH9 3HJ*

⁴*Anglo-Australian Observatory, PO Box 296, Epping, NSW 2121, Australia*

⁵*Research School of Astronomy & Astrophysics, The Australian National University, Weston Creek, ACT 2611, Australia*

⁶*Astrophysics Research Institute, Liverpool John Moores University, Twelve Quays House, Birkenhead L14 1LD*

⁷*Department of Astrophysics, University of New South Wales, Sydney, NSW 2052, Australia*

⁸*Department of Physics, University of Oxford, Keble Road, Oxford OX1 3RH*

⁹*School of Physics and Astronomy, University of St. Andrews, North Haugh, St. Andrews, Fife KY6 9SS*

¹⁰*Institute of Astronomy, University of Cambridge, Madingley Road, Cambridge CB3 0HA*

¹¹*Department of Astronomy, California Institute of Technology, Pasadena, CA 91125, USA*

¹²*Department of Physics & Astronomy, Johns Hopkins University, Baltimore, MD 21218-2686, USA*

¹³*Department of Physics, University of Leeds, Woodhouse Lane, Leeds LS2 9JT*

Accepted 2001 July 16. Received 2001 July 9; in original form 2001 May 30

ABSTRACT

We investigate the dependence of the strength of galaxy clustering on intrinsic luminosity using the Anglo-Australian two degree field galaxy redshift survey (2dFGRS). The 2dFGRS is over an order of magnitude larger than previous redshift surveys used to address this issue. We measure the projected two-point correlation function of galaxies in a series of volume-limited samples. The projected correlation function is free from any distortion of the clustering pattern induced by peculiar motions and is well described by a power law in pair separation over the range $0.1 < (r/h^{-1} \text{ Mpc}) < 10$. The clustering of $L^*(M_{b_j} - 5 \log_{10} h = -19.7)$ galaxies in real space is well-fitted by a correlation length $r_0 = 4.9 \pm 0.3 h^{-1} \text{ Mpc}$ and power-law slope $\gamma = 1.71 \pm 0.06$. The clustering amplitude increases slowly with absolute magnitude for galaxies fainter than M^* , but rises more strongly at higher luminosities. At low luminosities, our results agree with measurements from the Southern Sky Redshift Survey 2 by Benoist et al. However, we find a weaker dependence of clustering strength on luminosity at the highest luminosities. The correlation function amplitude increases by a factor of 4.0 between $M_{b_j} - 5 \log_{10} h = -18$ and -22.5 , and the most luminous galaxies are 3.0 times more strongly clustered than L^* galaxies. The power-law slope of the correlation function shows remarkably little variation for samples spanning a factor of 20 in luminosity. Our measurements are in very good agreement with the predictions of the hierarchical galaxy formation models of Benson et al.

Key words: methods: numerical – methods: statistical – galaxies: clusters: general – galaxies: formation – large-scale structure of Universe.

*E-mail: Peder.Norberg@durham.ac.uk

1 INTRODUCTION

A major obstacle to be overcome by any successful theory of the formation of large-scale structure is the problem of how galaxies trace the distribution of matter in the Universe. Measurements of differential galaxy clustering as a function of colour (Willmer, Da Costa & Pellegrini 1998), morphological type (Davis & Geller 1976; Iovino et al. 1993) and selection passband (Peacock 1997; Hoyle et al. 1999) imply the existence of biases between the distribution of galaxies and that of mass.

A generic prediction of hierarchical structure formation models is that rarer objects should be more strongly clustered than average (Davis et al. 1985; White et al. 1987). Correspondingly, if more luminous galaxies are associated with more massive haloes, then these galaxies are expected to exhibit stronger clustering than the galaxy population as a whole (for the special case of bright galaxies at high redshift, see for example Baugh et al. 1998; Governato et al. 1998). However, the form of the dependence of the amplitude of galaxy clustering on luminosity remains controversial even after more than 20 yr of constructing and analysing redshift surveys of the local Universe. In the literature, claims of a dependence of galaxy clustering on luminosity (e.g. Davis et al. 1988; Hamilton 1988; Maurogordato & Lachize-Rey 1991; Park et al. 1994; Benoist et al. 1996; Willmer et al. 1998; Guzzo et al. 2000) have been made with similar regularity to claims of non-detections (e.g. Phillips & Shanks 1987; Hasegawa & Umemura 1993; Loveday et al. 1995; Szapudi et al. 2000; Hawkins et al. 2001). Part of the reason for this disagreement is a mismatch in the range of luminosities and clustering length-scales considered in earlier studies. However, the main problem with earlier work is the small size of the redshift surveys analysed, in terms of both volume and number of galaxies. With previous surveys, the dynamic range in luminosity for which clustering can be reliably measured is limited, particularly when volume-limited samples are used. Because of the small volumes probed, it has generally not been possible to compare the clustering of galaxies of different luminosity measured within the same volume. These results have generally been affected by sampling fluctuations that are difficult to quantify. This problem is compounded by underestimation of the errors on the measured correlation functions and on the power-law fits traditionally employed in this subject.

In this paper, we use the largest extant local survey, the Anglo-Australian two degree field galaxy redshift survey (hereafter 2dFGRS), to address the issue of how clustering depends upon galaxy luminosity. We describe the 2dFGRS and the construction of volume-limited samples in Section 2, and our estimation of the correlation function is described in Section 3. Our results for the real-space correlation function are given in Section 4. We compare our results with those from previous studies and with the predictions of simulations of hierarchical galaxy formation in Section 5.

2 THE DATA

2.1 The 2dFGRS sample

The 2dFGRS is selected in the photometric b_j band from the automated plate measurement (APM) galaxy survey (Maddox et al. 1990a,b; 1996) and its subsequent extensions (Maddox et al. in preparation). The survey is divided into two regions and covers approximately 2000 deg^2 . The bulk of the solid angle of the survey is made up of two broad strips, one in the South Galactic Pole

(SGP) region covering approximately $-37.5 < \delta < -22.5$, $21^{\text{h}}40^{\text{m}} < \alpha < 3^{\text{h}}30^{\text{m}}$ and the other in the direction of the North Galactic Pole (NGP), spanning $-7.5 < \delta < 2.5$, $9^{\text{h}}50^{\text{m}} < \alpha < 14^{\text{h}}50^{\text{m}}$. In addition to these contiguous regions, there are a number of circular two-degree fields scattered pseudo-randomly over the full extent of the low extinction regions of the southern APM galaxy survey. In this paper, we use the redshifts obtained prior to 2001 January, over 160 000 in total. As we are mainly interested in measuring clustering out to separations of order $20 h^{-1} \text{ Mpc}$, we do not include galaxies that lie in the random fields in our analysis.

In order to select an optimal sample for the measurement of the two-point correlation function, we apply a weighting scheme to objects in the 2dFGRS. A weight is assigned to each measured redshift based upon the redshift completeness mask, the construction of which is explained in Colless et al. (2001; see also Norberg et al., in preparation). We require a relatively high completeness in a given direction on the sky, so that, in practice, our results are fairly insensitive to the precise details of the weighting scheme. Excluding areas below our completeness threshold (which arise mainly as a result of the tiling strategy adopted to make optimal use of telescope time, coupled with the fact that the survey is not yet finished), we estimate the effective solid angle used in the SGP region to be $\sim 420 \text{ deg}^2$, and in the NGP to be $\sim 190 \text{ deg}^2$.

2.2 Constructing a volume-limited sample

In this paper, we analyse a series of volume-limited subsamples drawn from the 2dFGRS. The advantage of this approach is that the radial selection function is uniform, and the only variations in the space density of galaxies within each volume are because of clustering. In contrast, in a flux-limited survey, the galaxy number density is a strong function of radial distance and this needs to be corrected for when measuring the clustering. The disadvantage of using a volume-limited sample is that a large number of galaxies in the flux-limited survey do *not* satisfy the selection cuts (which are explained below). This is a serious problem for previous surveys, but not for a survey which is of the size of the 2dFGRS. As we demonstrate in Section 4, the volume-limited samples we analyse give robust clustering measurements and contain over an order of magnitude more galaxies than similar samples constructed from previous surveys (see Table 1).

The construction of a volume-limited sample drawn from a flux-limited redshift survey requires a range of absolute magnitudes to be specified. Since a flux-limited survey has both bright and faint apparent magnitude limits, the selected range of absolute magnitudes requires that both a minimum (z_{min}) and a maximum (z_{max}) redshift cut be applied to the volume-limited sample. Thus, in principle, a galaxy included in the volume-limited sample could be displaced to any redshift between z_{min} and z_{max} and still remain within the bright and faint *apparent* magnitude limits of the flux-limited survey.

In order to estimate the absolute magnitude of 2dFGRS galaxies at redshift zero, it is necessary to apply corrections for band shifting (k -correction) and evolution in the stellar populations (e -correction). We adopt a global $k + e$ correction given by $k + e = 0.03z/(0.01 + z^4)$, which is a good fit to the correction calculated for the b_j selected European Southern Observatory (ESO) Slice Project survey using population synthesis models (see fig. 1 of Zucca et al. 1997). This form for the $k + e$ correction gives consistent luminosity functions for the 2dFGRS when the survey is divided into redshift bins, indicating that it adequately accounts for

Table 1. Properties of the combined NGP and SGP volume-limited subsamples analysed. The second column gives the median magnitude of each sample. Columns 6 and 7 list the best-fitting correlation length, r_0 , and power-law slope γ of the correlation function in real space, fitted over the range $0.5 \leq \sigma/(h^{-1} \text{Mpc}) \leq 10$. Column 8 gives the value of $A(\gamma)$, defined by equation (4), evaluated for the best-fitting value of γ .

Mag. range $M_{bj} - 5 \log_{10} h$	Median magnitude $M_{bj} - 5 \log_{10} h$	N_{gal}	z_{min}	z_{max}	r_0 ($h^{-1} \text{Mpc}$)	γ	$A(\gamma)$
-18.0 - 18.5	-18.11	7061	0.010	0.086	4.14 ± 0.64	1.78 ± 0.10	3.75
-18.5 - 19.0	-18.61	9382	0.013	0.104	4.43 ± 0.45	1.75 ± 0.08	3.80
-19.0 - 19.5	-19.11	13690	0.016	0.126	4.75 ± 0.44	1.68 ± 0.08	4.14
-19.5 - 20.0	-19.60	15123	0.020	0.152	4.92 ± 0.27	1.71 ± 0.06	4.01
-20.0 - 20.5	-20.09	13029	0.025	0.182	5.46 ± 0.28	1.68 ± 0.06	4.14
-20.5 - 21.0	-20.58	9114	0.031	0.220	6.49 ± 0.29	1.63 ± 0.06	4.39
-21.0 - 21.5	-21.06	3644	0.039	0.270	7.58 ± 0.48	1.76 ± 0.09	3.82
-18.0 - 19.0	-18.22	12594	0.013	0.086	4.06 ± 0.53	1.79 ± 0.09	3.72
-19.0 - 20.0	-19.19	21874	0.020	0.126	4.75 ± 0.44	1.70 ± 0.08	4.06
-20.0 - 21.0	-20.13	17383	0.031	0.182	5.65 ± 0.30	1.69 ± 0.06	4.10
-21.0 - 22.0	-21.07	4013	0.048	0.270	8.12 ± 0.46	1.78 ± 0.12	3.75
-21.5 - 22.5	-21.55	1002	0.059	0.280	9.38 ± 1.48	1.69 ± 0.15	4.10

the degree of evolution in galaxy luminosity over the look-back time spanned by the survey (Norberg et al., in preparation). Our results are unchanged if we use the mean of the k -corrections for different spectral types given by Madgwick et al. (2001). The values of z_{min} and z_{max} that define a volume-limited sample drawn from the 2dFGRS vary slightly with the position on the sky. This is because of the revisions made to the map of galactic extinction (Schlegel, Finkbeiner & Davis 1998) and to the CCD calibration of APM plate zero-points since the definition of the original input catalogue. Throughout the paper, we adopt an $\Omega_0 = 0.3$, $\Lambda_0 = 0.7$ cosmology to convert redshift into comoving distance.

3 ESTIMATING THE TWO-POINT CORRELATION FUNCTION

The galaxy correlation function is estimated on a two-dimensional grid of pair separations parallel (π) and perpendicular (σ) to the line of sight. To estimate the mean density of pairs, a catalogue of unclustered points is generated with the same angular selection and ($z_{\text{min}}, z_{\text{max}}$) values as the data. The correlation function is estimated by

$$\xi = \frac{DD - 2DR + RR}{RR}, \quad (1)$$

where DD , DR and RR are the suitably normalized number of weighted data–data, data–random and random–random pairs, respectively in each bin (Landy & Szalay 1993).

Contours of constant clustering amplitude in the redshift-space correlation function, $\xi(\sigma, \pi)$, are distorted as a result of the peculiar motions of galaxies, as demonstrated for the 2dFGRS by Peacock et al. (2001). On small scales, random motions inside virialized structures elongate the constant- ξ contours in the π direction, whereas on large scales, coherent flows flatten the contours. The latter effect was measured clearly for the first time for galaxies using the 2dFGRS (Peacock et al. 2001). The dependence of the redshift-space correlation function on galaxy luminosity is analysed in a separate paper (Hawkins et al., in preparation). In this paper, to simplify the interpretation, we consider only clustering in real space, which we infer by projecting the measured correlation function along the line of sight. We compute a

dimensionless quantity, $\Xi(\sigma)/\sigma$, by integrating over the measured $\xi(\sigma, \pi)$ grid (note that $\Xi(\sigma)$ is sometimes referred to as $w(r_p)$ in the literature):

$$\frac{\Xi(\sigma)}{\sigma} = \frac{1}{\sigma} \int_{-\infty}^{\infty} \xi(\sigma, \pi) d\pi. \quad (2)$$

In practice, the integral converges by a pair separation of $\pi = 75 h^{-1} \text{Mpc}$. The projected correlation function can, in turn, be written as an integral over the spherically averaged real-space correlation function, $\xi(r)$,

$$\frac{\Xi(\sigma)}{\sigma} = \frac{2}{\sigma} \int_{\sigma}^{\infty} \xi(r) \frac{r dr}{(r^2 - \sigma^2)^{1/2}}, \quad (3)$$

(Davis & Peebles 1983). If the real-space correlation function is a power law (which is a reasonable approximation for APM galaxies out to separations around $r \sim 10 h^{-1} \text{Mpc}$, see e.g. Baugh 1996), then

$$\frac{\Xi(\sigma)}{\sigma} = \left(\frac{r_0}{\sigma}\right)^{\gamma} \frac{\Gamma(1/2)\Gamma[(\gamma-1)/2]}{\Gamma(\gamma/2)} = \left(\frac{r_0}{\sigma}\right)^{\gamma} A(\gamma), \quad (4)$$

where $\xi(r) = (r_0/r)^{\gamma}$ and r_0 is the correlation length.

Previous studies have estimated the error on the measured correlation function from the Poisson statistics of the pair counts in each bin (Peebles 1980) or by bootstrap resampling of the data (e.g. Benoist et al. 1996). Since we study a range of samples corresponding to different luminosity bins and also compare samples from different volumes, it is important to include an estimate of the sampling fluctuations in the error budget for the correlation function. This we derive from an analysis of 22 mock 2dFGRS catalogues constructed from the Λ CDM Hubble Volume dark matter simulation, in the manner explained by Baugh et al. (in preparation; see also Cole et al. 1998). In order to mimic the clustering of the 2dFGRS, a biasing scheme is employed to select particles in the simulations with a probability which is a function of the final dark matter density field, smoothed with a Gaussian filter (model 2 of Cole et al. 1998). The mock catalogues have the same clustering amplitude as galaxies in the flux-limited 2dFGRS, and the same selection criteria that are applied to the data are used in the construction of the mock surveys. The clustering amplitude in the mocks is independent of luminosity. The error bars that we plot

on correlation functions measured from the 2dFGRS are the rms found by averaging over the 22 mock catalogues.

4 RESULTS

We first demonstrate the robustness of the approach of measuring the correlation function in volume-limited samples. Unless stated otherwise, we have added the pair counts in the NGP and SGP regions to compute correlation functions. In Fig. 1(a), we show the correlation function of galaxies in three disjoint absolute magnitude bins measured in the same volume. The sampling fluctuations are therefore virtually the same for each subsample, although the number of galaxies varies between them. There is a clear difference in the clustering amplitude of galaxies in the brightest absolute magnitude bin. Next, we demonstrate that sampling fluctuations are not important in a survey which is of the size of the 2dFGRS. We show, in Fig. 1(b), the correlation function in two fixed absolute magnitude bins measured in different volume-limited subsamples. Specifically, the dashed lines show the

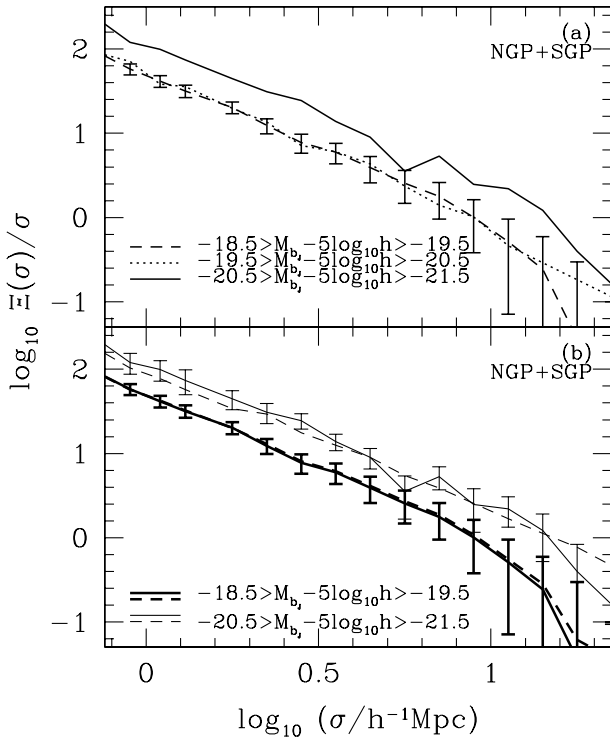


Figure 1. (a) The projected correlation function measured for galaxies in three different absolute magnitude bins in the *same* volume. The faintest sample contains 16 134 galaxies, the middle sample contains 6 186 galaxies and the brightest sample contains 985 galaxies. For clarity, error bars are plotted only on the correlation function of galaxies with $-18.5 \geq M_{bj} - 5 \log_{10} h \geq -19.5$. (b) A comparison of the correlation function of galaxies in the same absolute magnitude bins but measured in different (although not completely independent) volumes. The heavy lines show results for galaxies with $-18.5 \geq M_{bj} - 5 \log_{10} h \geq -19.5$ and the light lines show results for a brighter bin with $-20.5 \geq M_{bj} - 5 \log_{10} h \geq -21.5$. In each case, the dashed line shows the estimate from the optimal sample (see text) for the selected magnitude bin, whilst the solid line shows an estimate of the correlation function from the volume analysed in Fig. 1(a). For the $-20.5 \geq M_{bj} - 5 \log_{10} h \geq -21.5$ magnitude bin, the optimal estimate is measured using 10 962 galaxies, which should be contrasted with the 985 galaxies used to make the measurement shown by the light solid line, in a volume defined by a broader magnitude bin.

correlation function for the optimal volume-limited sample, appropriate to the selected absolute magnitude bin. Such a sample contains the maximum number of galaxies in that magnitude bin. The different estimates of the correlation function agree within the errors.

We now focus attention on the series of volume-limited subsamples covering the range $-18 \geq M_{bj} - 5 \log_{10} h \geq -22.5$, whose characteristics are listed in Table 1. The shape and amplitude of the projected correlation function in a selection of these samples are compared in Fig. 2 with the correlation function of galaxies in the magnitude range $-19 \geq M_{bj} - 5 \log_{10} h \geq -20$. The shape of the correlation function varies relatively little with the absolute magnitude that defines the sample in contrast to the amplitude of the correlation function, which changes significantly for the brightest magnitude slice. Another view of this trend is given in Fig. 3(a) where we plot the real-space correlation length as a function of absolute magnitude. The best-fitting values of the correlation length, r_0 , and power-law slope γ , are determined by applying equation (4) to the measured correlation function over the pair separation range $0.5 \leq \sigma/(h^{-1} \text{Mpc}) \leq 10$ and carrying out a χ^2 minimization. This simple χ^2 approach will not, however, give reliable estimates of the errors on the fitted parameters because of the correlation between the estimates at differing pair separations. We use the mock 2dFGRS catalogues to estimate the errors on the fitted parameters. In brief, the best-fitting values of r_0 and γ are found for each mock individually, using the simple χ^2 analysis. The estimated error bar is the rms scatter in the fitted parameters over the ensemble of mock catalogues.

In Fig. 3(a), we plot the correlation lengths for the NGP and SGP regions separately. These independent estimates are in excellent agreement with one another. The slope of the best-fitting power-law correlation function, given in Table 1, is similar for all the volume-limited samples considered. The clustering amplitude increases slowly with luminosity for galaxies fainter than M^*

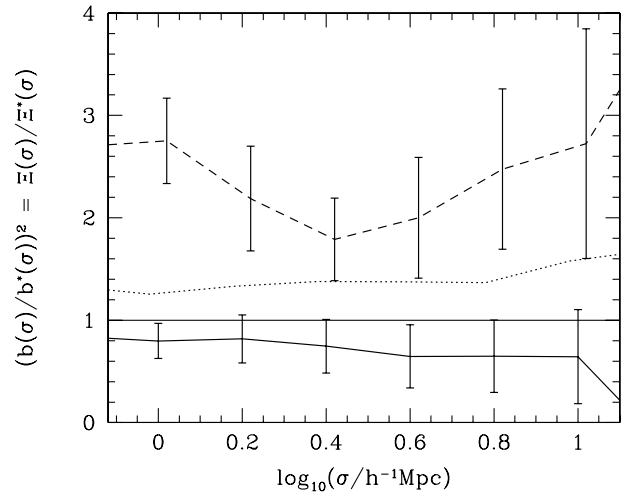


Figure 2. The ratio of the projected correlation function of galaxies in different magnitude slices to the projected correlation function of galaxies with $-19 \geq M_{bj} - 5 \log_{10} h \geq -20$. Note that the ratio is plotted on a linear scale, whilst the pair separation is on a log scale. The solid line shows the ratio for galaxies with absolute magnitudes in the range $-18 \geq M_{bj} - 5 \log_{10} h \geq -19$, the dotted line for $-20 \geq M_{bj} - 5 \log_{10} h \geq -21$, and the dashed line for $-21 \geq M_{bj} - 5 \log_{10} h \geq -22$. For clarity, error bars have been omitted from the dotted line but these are comparable in size with those plotted on the solid line.

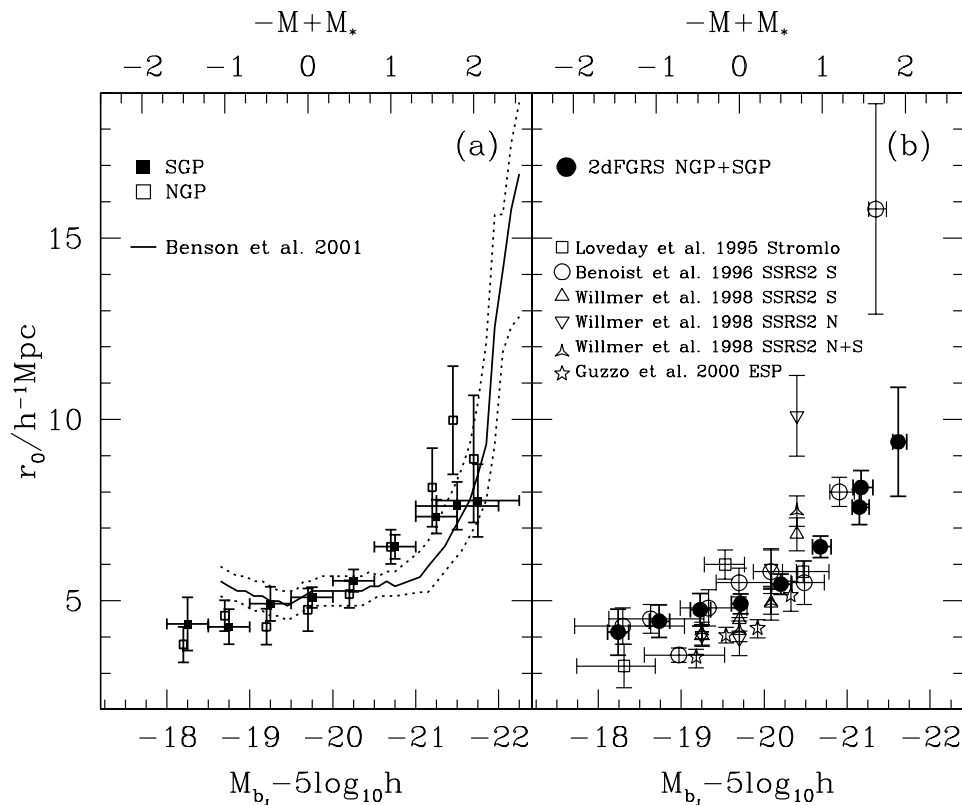


Figure 3. (a) The correlation length in real space as a function of absolute magnitude. Results are shown for the SGP and NGP regions separately. The NGP points are plotted with an offset of 0.05 mag for clarity. Horizontal error bars on the SGP points indicate the absolute magnitude range of each bin, and each point is plotted at the bin centre. In both cases, the brightest data points are for galaxies in 1-mag wide bins. The solid line shows the predictions of the semi-analytic model of Benson et al. (2001), computed in a series of overlapping bins, each 0.5 mag wide. The dotted curves show an estimate of the errors on this prediction, including the sample variance expected for a volume equal to that of the N -body simulation used. (b) The real-space correlation length estimated combining pairs counts in the NGP and SGP (filled circles). The open symbols show a selection of recent data from other studies. The data for surveys selected in the B band have been corrected to the b_j band using the approximate relation $M_{b_j} = M_B - 0.2$. In order to compare samples defined by cumulative and differential magnitude bins, the data points are plotted at the median magnitude of each sample.

(where $M^* = M_{b_j} - 5 \log_{10} h = -19.7$, as found by Folkes et al. 1999), but rises strongly at higher luminosities. The correlation function amplitude increases by a factor of 4.0 between $M_{b_j} - 5 \log_{10} h = -18$ and -22.5 , and the most luminous galaxies are 3.0 times more strongly clustered than M^* galaxies.

5 DISCUSSION

The volume-limited samples analysed in this paper contain over an order of magnitude more galaxies than previous studies of the dependence of clustering on galaxy luminosity, allowing a more accurate measurement of this effect than was possible before. The sheer volume covered by our samples, $10^6 - 2 \times 10^7 h^{-3} \text{Mpc}^3$, ensures that sampling fluctuations have little impact upon our results.

We compare the 2dFGRS results with a selection of recent measurements taken from the literature since 1995 in Fig. 3(b). To compare samples defined by cumulative and differential magnitude bins, we plot the data points at the median magnitude for the sample, as computed using the Schechter function parameters for the 2dFGRS (Folkes et al. 1999). The horizontal bars plotted on selected points show the quartile range of the magnitude distribution in the sample. Benoist et al. (1996) analysed quasi-volume-limited samples in the SGP region of the Southern Sky Redshift Survey 2 (SSRS2), and found a sharp increase in the

correlation length for galaxies brighter than $M_B - 5 \log_{10} h = -20.5$. The Benoist et al. correlation lengths are measured in redshift space, although the authors report that a similar trend with luminosity is seen in real space. Willmer et al. (1998) re-analysed the SSRS2 South using different volume limits and also measured clustering in the SSRS2 North, presenting fits for the correlation length in real and redshift space. Intriguingly, Willmer et al. find a larger correlation length in real space for galaxies with $M_B - 5 \log_{10} h \sim -20$ than that found by Benoist et al. in redshift space. Moreover, the clear disagreement between the results for the brightest galaxies analysed in SSRS2 North and South suggests that sampling fluctuations are significant in a survey of this size and that the errors on these points have been underestimated (as demonstrated in fig. 4 of Benson et al. 2001). Loveday et al. (1995) measured the clustering in real space by cross-correlating galaxies in the sparsely sampled Stromlo/APM redshift survey with galaxies in the parent catalogue. Galaxies were considered in three absolute magnitude bins. No difference was found between the clustering amplitude of L^* and super- L^* galaxies. However, the median magnitude for the most luminous sample considered by these authors is only 0.5 mag brighter than M^* . The increase in clustering amplitude with luminosity is connected with a change in the mix of morphological types with increasing luminosity. The mix of spectral types at the brightest absolute magnitudes is dominated by spectra characteristic of elliptical galaxies, whereas

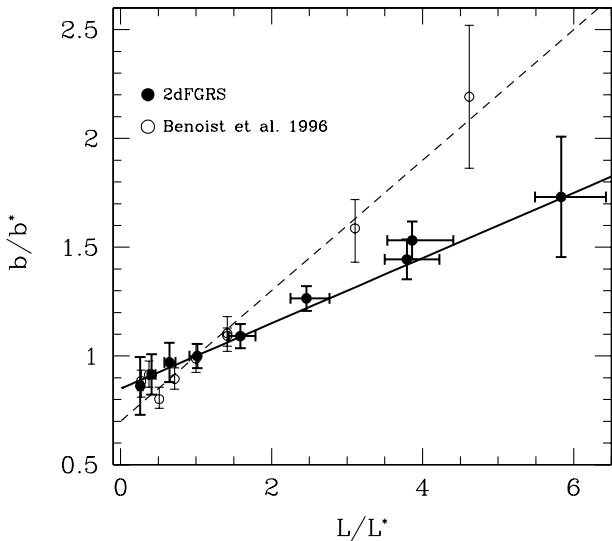


Figure 4. The variation of the relative bias as a function of luminosity using the clustering of L^* galaxies as a reference point (see text for definition). The 2dFGRS points are plotted at the median magnitude of each sample and the horizontal bars show the quartile magnitude range. The Benoist et al. (1996) points are taken from their fig. 5 and are plotted at the median value of L/L^* for each sample. Note that the error bars on the Benoist et al. points are obtained by averaging over correlated bins in pair separation. The curves show parametric fits: the Benoist et al. measurements are well fitted by $b/b^* = 0.7 + 0.3L/L^*$ (dashed line), whereas the 2dFGRS results suggest a more modest dependence on luminosity: $b/b^* = 0.85 + 0.15L/L^*$ (solid line).

spiral galaxies are more numerous around L^* (Folkes et al. 1999; Cole et al. 2001; Madgwick et al. 2001). The clustering of galaxies as a function of spectral type will be analysed in a separate paper.

Our clustering results can be characterized in a concise way in terms of a relative bias parameter, b/b^* , that gives the amplitude of the correlation function relative to that of L^* galaxies (where $M^* = M_{b_j} - 5 \log_{10} h = -19.7$). The relative bias between the correlation functions of galaxies of different luminosity is assumed to be constant for pair separations spanned by the r_0 values listed in Table 1 (see also Fig. 2). The relative bias is then defined by $b/b^* = (r_0/r_0^*)^{\gamma/2}$, where we take $r_0^* = 4.9 \pm 0.3 h^{-1}$ Mpc from Table 1 and use $\gamma = 1.7$. The 2dFGRS results are shown by the filled symbols in Fig. 4 and are well fitted by the relation $b/b^* = 0.85 + 0.15L/L^*$. The 2dFGRS data suggest a significantly weaker dependence of the relative bias on luminosity than the Benoist et al. data, which follow the relation $b/b^* = 0.7 + 0.3L/L^*$ (Peacock et al. 2001). (The parametric fit to the Benoist et al. measurements was used by Peacock et al. 2001 to estimate the parameter $\beta = \Omega^{0.6}/b$ for L^* galaxies in the 2dFGRS. Using the above fit to the 2dFGRS measurements changes the inferred value for β by less than 1σ to $\beta = 0.49 \pm 0.08$.)

Hierarchical models of galaxy formation predict that bright galaxies should be more strongly clustered than faint galaxies (e.g. White et al. 1987; Kauffmann, Nusser & Steinmetz 1997). This generic prediction arises because bright galaxies are expected to occupy more massive dark matter haloes and these haloes are more strongly clustered than the overall distribution of dark matter. The trend of clustering amplitude with luminosity measured for 2dFGRS galaxies is in very good agreement with the predictions of a simulation of hierarchical galaxy formation taken from fig. 4 of Benson et al. (2001), reproduced as the solid line in Fig. 3(a). In the

Benson et al. semi-analytic model, the input parameters are set in order to reproduce a subset of local galaxy data, with most emphasis given to the field galaxy luminosity function (see Cole et al. 2000). No reference is made to clustering data in setting the model parameters. In a Λ CDM cosmology, Benson et al. (2000a,b) find excellent agreement with the real-space correlation function measured for galaxies in the APM survey by Baugh (1996). It is remarkable that the same model, without any readjustment of parameters, also reproduces the dependence of clustering amplitude on luminosity exhibited by the 2dFGRS in Fig. 3(a).

ACKNOWLEDGMENTS

The 2dFGRS is being carried out using the two-degree field facility on the 3.9-m Anglo-Australian Telescope (AAT). We thank all those involved in the smooth running and continued success of the 2dF and the AAT. We thank the referee, Dr. L. Guzzo, for producing a speedy and helpful report, and also Andrew Benson for communicating an electronic version of his model predictions. PN was supported by the Swiss National Science Foundation and an ORS award and CMB acknowledges receipt of a Royal Society University Research Fellowship. This work was supported in part by a PPARC rolling grant at Durham.

REFERENCES

- Baugh C. M., 1996, MNRAS, 280, 267
 Baugh C. M., Cole S., Frenk C. S., Lacey C. G., 1998, ApJ, 498, 504
 Benoist C., Maurogordato S., Da Costa L. N., Cappi A., Schaeffer R., 1996, ApJ, 472, 452
 Benson A. J., Baugh C. M., Cole S., Frenk C. S., Lacey C. G., 2000a, MNRAS, 316, 107
 Benson A. J., Cole S., Frenk C. S., Baugh C. M., Lacey C. G., 2000b, MNRAS, 311, 793
 Benson A. J., Frenk C. S., Baugh C. M., Cole S., Lacey C. G., 2001, MNRAS, submitted, astro-ph/0103092
 Cole S., Hatton S., Weinberg D. H., Frenk C. S., 1998, MNRAS, 300, 945
 Cole S., Lacey C. G., Baugh C. M., Frenk C. S., 2000, MNRAS, 319, 168
 Cole S. et al. (the 2dFGRS team), 2001, MNRAS, 326, 255
 Colless M. et al. (the 2dFGRS team), 2001, MNRAS, in press, astro-ph/0106498
 Davis M., Geller M. J., 1976, ApJ, 208, 13
 Davis M., Peebles P. J. E., 1983, ApJ, 267, 465
 Davis M., Efstathiou G., Frenk C. S., White S. D. M., 1985, ApJ, 292, 371
 Davis M., Meiksin A., Strauss M. A., Da Costa L. N., Yahil A., 1988, ApJ, 33, L9
 Folkes S. et al. (the 2dFGRS team), 1999, MNRAS, 308, 459
 Governato F., Baugh C. M., Frenk C. S., Cole S., Lacey C. G., Quinn T., Stadel J., 1998, Nat, 392, 359
 Guzzo L. et al., 2000, A&A, 355, 1
 Hamilton A. J. S., 1988, ApJ, 331, L59
 Hasegawa T., Umemura M., 1993, MNRAS, 263, 191
 Hawkins E., Maddox S. J., Branchini E., Saunders W., 2001, MNRAS, 325, 589
 Hoyle F., Baugh C. M., Shanks T., Ratcliffe A., 1999, MNRAS, 309, 659
 Iovino A., Giovanelli R., Haynes M., Chincarini G., Guzzo L., 1993, MNRAS, 265, 21
 Kauffmann G., Nusser A., Steinmetz M., 1997, MNRAS, 286, 795
 Landy S. D., Szalay A. S., 1993, ApJ, 412, 64
 Loveday J., Maddox S. J., Efstathiou G., Peterson B. A., 1995, ApJ, 442, 457
 Maddox S. J., Efstathiou G., Sutherland W. J., Loveday J., 1990a, MNRAS, 243, 692
 Maddox S. J., Efstathiou G., Sutherland W. J., Loveday J., 1990b, MNRAS, 246, 433

- Maddox S. J., Efstathiou G., Sutherland W. J., Loveday J., 1996, *MNRAS*, 283, 1227
- Madgwick D. et al. (the 2dFGRS team), 2001, *MNRAS*, submitted
- Maurogordato S., Lachieze-Rey M., 1991, *ApJ*, 369, 30
- Park C., Vogeley M. S., Geller M. J., Huchra J. P., 1994, *ApJ*, 431, 569
- Peacock J. A., 1997, *MNRAS*, 284, 885
- Peacock J. A. et al. (the 2dFGRS team), 2001, *Nat*, 410, 169
- Peebles P. J. E., 1980, *The Large Scale Structure of the Universe*. Princeton Univ. Press, Princeton
- Phillips S., Shanks T., 1987, *MNRAS*, 229, 621
- Schlegel D. J., Finkbeiner D. P., Davis M., 1998, *ApJ*, 500, 525
- Szapudi I., Branchini E., Frenk C. S., Maddox S., Saunders W., 2000, *MNRAS*, 318, L45
- White S. D. M., Davis M., Efstathiou G., Frenk C. S., 1987, *Nat*, 330, 351
- Willmer C. N. A., Da Costa L. N., Pellegrini P. S., 1998, *AJ*, 115, 869
- Zucca E. et al., 1997, *A&A*, 326, 477

This paper has been typeset from a \TeX/L\AA\TeX file prepared by the author.